ВЫСШИЕ УЧЕБНЫЕ ЗАВЕДЕНИЯ

UDC 539.3

SHERBAKOV Sergei S., D. Sc. in Phys. and Math., Assoc. Prof.
Professor of the Department of Theoretical and Applied Mechanics[1]
E-mail: sherbakovss@mail.ru

SHI Wu, Assoc. Prof.
Associate Professor of the School of Mechanical and Power Engineering[2]
E-mail: wushi971819@163.com

JUNPENG Shao, Prof.
Dean of the School of Mechanical and Power Engineering[2]
E-mail: sjp566@hrbust.edu.cn

NASAN Aleh A.
Junior Researcher[1]
E-mail: nasan_o@mail.ru

[1]Belarusian State University, Minsk, Republic of Belarus
[2]Harbin University of Science and Technology, Harbin, China

Received 05 July 2017.

SPATIAL STRESS-STRAIN STATE OF BORING BAR FRONT-END STRUCTURE OF HEAVY-DUTY HORIZONTAL BORING LATHE

Mechanical and mathematical models describing the spatial stress-strain state and frictional contacts between elastic elements of the boring bar front-end structure of heavy-duty horizontal boring lathe were developed. All the calculations were performed using the finite element simulation package ANSYS Workbench Mechanical. Static formulation of the problem with the account of gravitational force and non-linear behavior of the materials in the vicinity of the cutting surface of the cutter was considered. Four different statements of the problem were analyzed. They illustrate the effect of the bolted connections pretension clamping the cutter on the stress-strain state of the system. The effect of front-end structure's loading on the boring bar during cutting was investigated. The effect of the boring bar bending on front-end structure was analyzed. The carried out analysis showed that the components of the stress-strain state of the studied systems have similar distributions, regardless to the bending of the boring bar due to the force of gravity. Bending of the boring bar has significant influence only on the displacements. Stress concentrators were present in many regions of the studied system. This complicated the analysis of complex distributions of stresses and strains fields. Obtained results demonstrate the need of movement from the local characteristics of damageability (stress tensor components) to the integral ones – dangerous volumes.

Keywords: *tribo-fatigue, multi-element system, stress-strain state, finite element modeling, heavy-duty boring lathe, boring bar, front-end structure*

Problem statement. The object of study is multi-element tribo-fatigue boring bar front-end support system, which is one of the most critical components of heavy-duty horizontal boring lathe shown in figure 1. Multiple contact interactions with friction between its various elements and a non-contact bending of the boring bar occur in this system [1–9].

The purpose of work is the development of mechanical and mathematical models allowing description of the three-dimensional stress-strain state and multiple contact interaction of the elastic elements of the boring bar front-end support system.

The main methods of research are the ones of tribo-fatigue, solid mechanics and computational mechanics.

Figure 1 — Heavy-duty horizontal boring lathe

The boring bar has the shape of a hollow cylinder with an outer radius of 200 mm and inner radius of 150 mm. Its loading scheme is shown on the figure 2.

Points *A*, *B*, *C*, *D* and *E* are the starting points of the areas fixed in all directions, $l_{I\text{-}J}$ is the distance from the beginning of the section *I* to the beginning of the section *J*, *d* is the length of the front-end system of boring bar. The values of all the parameters are presented in table 1.

The front-end support structure of the boring bar consists of the upper support (1) where cutter is placed, middle support (2), the lower support (3) and the boring bar (4) (see figure 3).

The elements of the front-end support structure of the boring bar are connected by the groups of bolts shown in figure 4.

Within the current study four different calculations were made. Effect of bolts pretension clamping the cutter as well as the impact of boring bar were considered (see figure 5). The codification of these calculations is shown in table 2 and mechanical characteristics of the materials used [10] are given in table 3.

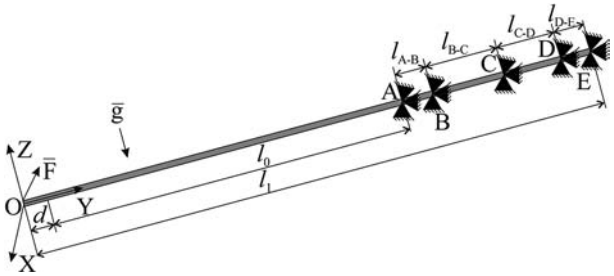

Figure 2 — Boring bar loading scheme

Table 1 — Sections length

Section Name	Length, mm
A	540
B	540
C	540
D	540
E	468
$l_{A\text{-}B}$	1260
$l_{B\text{-}C}$	2703,8
$l_{C\text{-}D}$	3108
$l_{D\text{-}E}$	1400
d	166,7
l_0	6488,2
l_1	15596,7

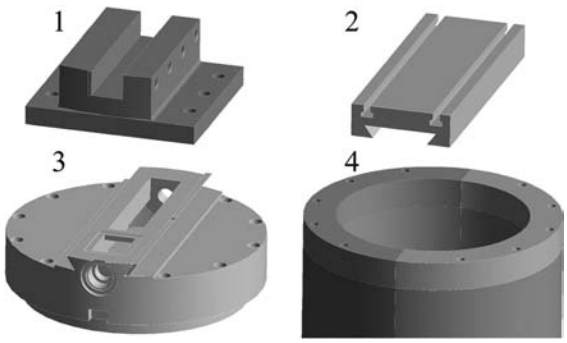

Figure 3 — Elements of the boring bar front-end support system

Suppose that $\mathbf{r}^k$ is the particular configuration of the *k*-th body in space for calculated system (see figures 5, 6). In this case the following relations that determine the mechanical state of the particle of the body (the elementary volume) can be formulated: the continuity equation, the equations of equilibrium of the body's particles, dependency between displacements and strains, and Hooke's law [4, 9].

Boundary conditions of the first type for the surfaces S_u of the front-end support base of the boring bar where displacements $\overline{u}_i^{k*}\left(\mathbf{r}^k\right)$ are set in calculations *H* and *HN* (see figure 6) are added to the equations that determine the mechanical state:

$$u_i^k = \overline{u}_i^{k*}\left(\mathbf{r}^k\right),\ i = x, y, z, \tag{1}$$

and boundary conditions of the second type for the surfaces S_σ of other elements of the system where the distributions of tractions $\overline{p}_i$ are set (see figures 5, 6):

$$\sigma_{ij}^k \alpha_j^k = \overline{p}_i^k\left(\overline{\mathbf{F}}_N, \mathbf{r}^k\right), \tag{2}$$

where α_j^k are the direction cosines.

Interaction of the elements of the system consisting from *n* deformable bodies can be described using the

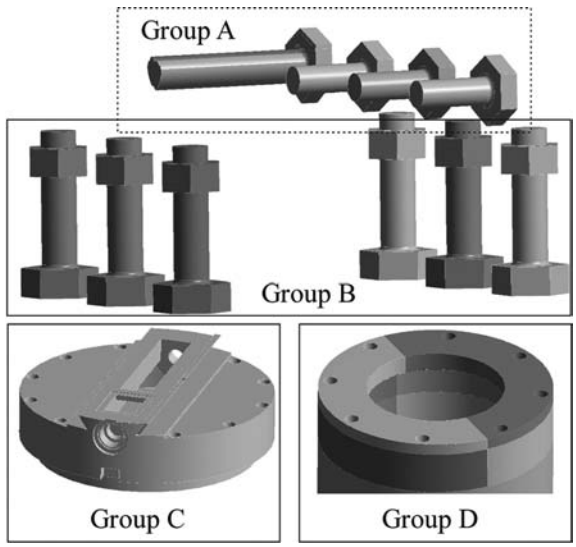

Figure 4 — Groups of bolted connections

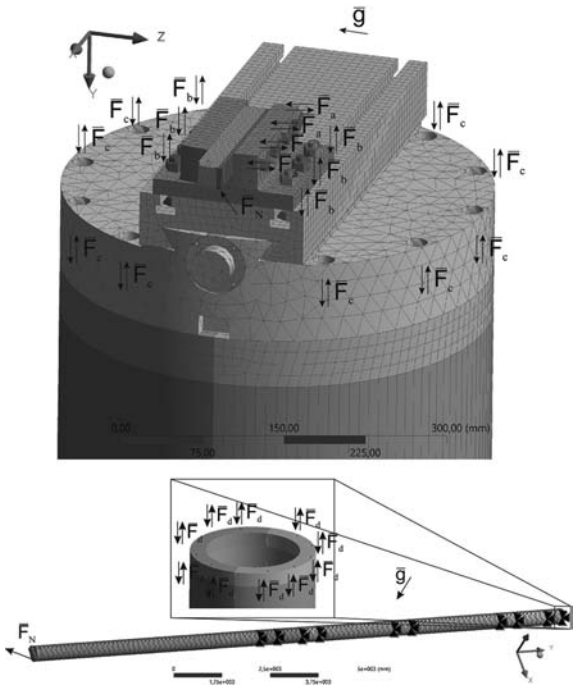

Figure 5 — Finite element mesh and loading scheme for calculations *FN* and *F*

Table 2 — Codification of calculations

Loading conditions	Boring bar with loosed bolts holding the cutter	Boring bar with tightened bolts holding the cutter	Front-end support with loosed bolts holding the cutter	Front-end support with tightened bolts holding the cutter
Calculation's code	FN	F	HN	H

contact boundary conditions defined by the following relationships:

$$\overline{\mathbf{u}}_l\big|_{S_u^{(lm)}} - \overline{\mathbf{u}}_m\big|_{S_u^{(lm)}} = \boldsymbol{\delta}_{lm}^{(u)}\left(f_{lm}, \mathbf{r}^l, \mathbf{r}^m, t\right)\Big|_{S_u^{(lm)}}, \quad (3)$$

$$\overline{\mathbf{p}}_l\big|_{S_\sigma^{(lm)}} - \overline{\mathbf{p}}_m\big|_{S_\sigma^{(lm)}} = \boldsymbol{\delta}_{lm}^{(\sigma)}\left(f_{lm}, \mathbf{r}^l, \mathbf{r}^m, t\right)\Big|_{S_u^{(lm)}}, \quad (4)$$

where $S^{(lm)}$ are contact surfaces for bodies l and m, $S_\sigma^{(lm)} \subset S^{(lm)}$, $S_u^{(lm)} \subset S^{(lm)}$, $\overline{\mathbf{p}}_k = \left\{\overline{p}_1^k, \overline{p}_2^k, \overline{p}_3^k\right\} = \left\{p_n^k, p_{\tau 1}^k, p_{\tau 2}^k\right\}$ and $\overline{\mathbf{u}}_k = \left\{\overline{u}_1^k, \overline{u}_2^k, \overline{u}_3^k\right\}$ are vectors of tractions and displacements on the surface of k-th body, $p_n^k, p_{\tau 1}^k, p_{\tau 2}^k$ are normal and tangential components of surface tractions, $\boldsymbol{\delta}_{lm}^{(u)} = \{\delta_{lm}^{(n,u)}, \delta_{lm}^{(\tau 1,u)}, \delta_{lm}^{(\tau 2,u)}\}$, $\boldsymbol{\delta}_{lm}^{(\sigma)} = \{\delta_{lm}^{(n,\sigma)}, \delta_{lm}^{(\tau 1,\sigma)}, \delta_{lm}^{(\tau 2,\sigma)}\}$ are vectors of displacements and tractions on the contact surfaces, f_{lm} are friction coefficients for the corresponding pairs of bodies.

Table 3 — Mechanical properties

Material	Poisson's Ratio, ν	Young's modulus, *E*, GPa	Yield strength, $\sigma_т$, MPa	Strength limit, $\sigma_в$, MPa
Steel 18HGT, (for bolts)	0,3	211	885	980
Steel 18HGT	0,3	211	730	980

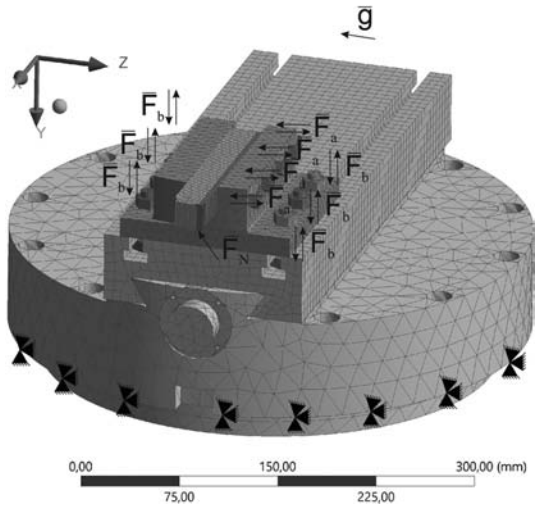

Figure 6 — Finite element mesh and loading scheme for calculations *HN* and *H*

Calculations *F* and *H* describe the behavior of the front-end support of the boring bar for the bolts of group *A* clamping the cutter by maximal bolts pretension force F_a = 24949,5 N (see table 4 and figure 4). Calculations *FN* and *HN* describe the behavior of the front-end support under absent bolts pretension force $F_a = 0$.

Friction coefficient *f* equals 0,18 for all calculations.

Methodology described in [11, 12] was used for the calculation of bolts pretension force (see table 3). Main assumption for this calculation is that this force should produce stresses in the bolts which do not surpass the yield limit.

Finite-element models with applied boundary conditions are shown in figures 5, 6. For a correct comparison of the obtained results calculations *H* and *HN* were performed using the same mesh in the vicinity of the front-end support of the boring bar as in calculations *FN* and *F*.

Cutting load was defined according to the data provided by Harbin University of Science and Technology: $\overline{F}_N = \{-3118; 3619; -8620\}$ *N*. Force $\overline{F}_N$ was applied to the three external faces of 4 mm length of the cutter.

All calculations were performed in the finite element simulation program package ANSYS Workbench in static formulation considering gravitational force field and non-linear behavior of the materials in the vicinity of the cutting surface of the cutter.

The calculations for all models were divided into two steps: the first step took into account the bolts pretension, the second one — cutting load.

Table 4 — Bolts pretension forces

Screw type	Group	Bolt pretension, *N*
M8x1 – 6g	*A*	F_a = 24949,5
M10x1 – 6g	*B*	F_b = 43048,7
M14x1,5 – 6g	*C*	F_c = 82341,3
M24x2 – 6g	*D*	F_d = 264903

At the second step the distribution of forces and displacements produced by bolts pretension were applied as the boundary conditions.

Stress-strain state of full models. In all calculations before cutting maximum von-Mises stress σ_{eqv} values were concentrated in the vicinity of the bolted connections of group *B* (see figures 4, 7, 8). Such high values (about 1,7 GPa for all calculations) are caused by rather coarse mesh of the fillet under the bolt head.

During cutting the maximum stresses occur on the cutting surfaces of the cutter while stresses of the bolted connections of group *B* remain almost unchanged. Outside the region of the bolted connections of group *B* σ_{eqv} do not exceed materials yield limit.

Comparison of von-Mises stress σ_{eqv} for calculations with boring bar (*FN* and *F*) bending and without it (*HN* and *H*) showed the same distribution pattern in the cutter, upper and middle supports, bolts of *A* and *B* groups for the same pretension of group *A* bolts. Only lower support has different σ_{eqv} distribution due to boring bar bending (see figures 7, 8).

Pretension of group *A* bolts does not change the position of the maximal of von-Mises stress but causes significant increase of σ_{eqv} in the upper support and the cutter.

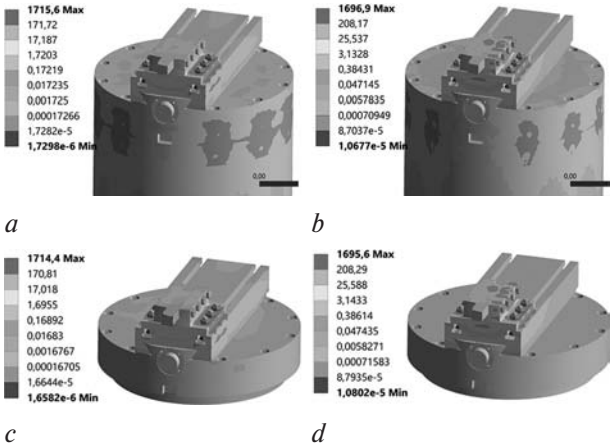

Figure 7 — Distribution of von-Mises stress seqv after the first loading step bolts (pretension): *a — FN*; *b — F*; *c — HN*; *d — H*, MPa

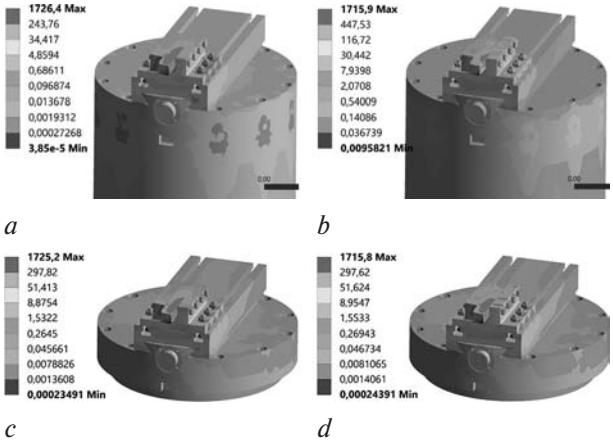

Figure 8 — Distribution of von-Mises stress seqv after the second loading step (cutting): *a — FN*; *b — F*; *c — HN*; *d — H*, MPa

Distributions of von-Mises strain ε_{eqv} have the pattern similar to the distributions of von-Mises stress (see figures 9, 10).

In all calculations after bolts pretension the cutter moves along the *x* axis with the displacement u_x ranging from 0,007 mm (calculations *F*, *H*) to 0,01 mm (calculations *FN*, *HN*) (see figure 11). During cutting the largest displacements in the system occur in calculations *F* (–1,67 mm) and *FN* (–1,68mm). In both these calculations motion of all parts of the system occurs in the negative direction along the *x* axis which is caused by the bending of boring bar (see figure 12). Rotation of the cutter counterclockwise about the *z* axis occurs in calculations *H* and *HN* during cutting.

Due to the lack of symmetry in the supports and mainly due to the impact of gravity after bolts pretension the whole front-end support system experienced rotation about the *x* axis counterclockwise which follows from the distribution of displacements u_y and u_z (see figures 13–16). Maximal u_z displacements in this case are 5,85 mm and 5,94 mm for *FN* and *F* calculations respectively. During cutting maximal displacements u_z are 10,86 mm and 10,9 mm for *FN* and *F* calculations respectively.

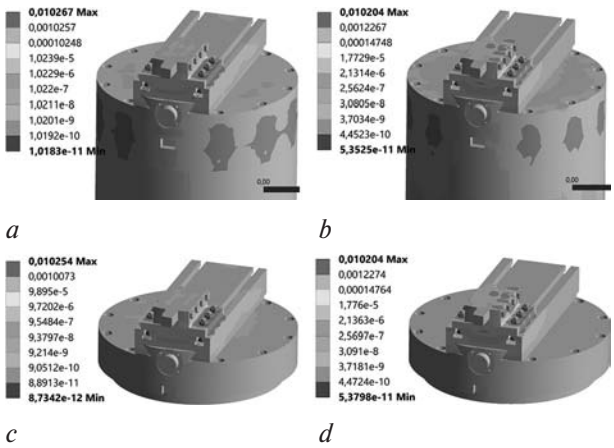

Figure 9 — Distribution of von-Mises strain eeqv after the first loading step (pretension): *a — FN*; *b — F*; *c — HN*; *d — H*

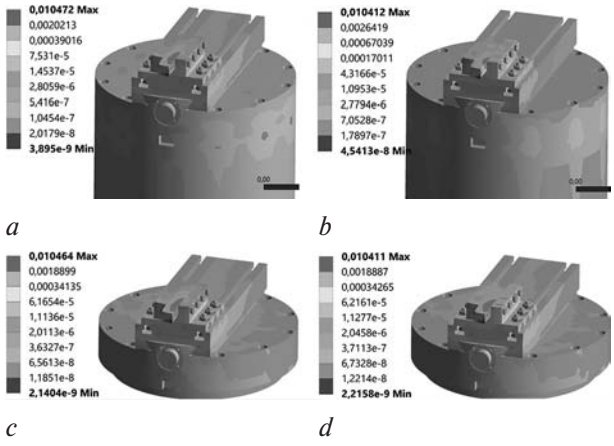

Figure 10 — Distribution of von-Mises strain eeqv after the second loading step (cutting): *a — FN*; *b — F*; *c — HN*; *d — H*

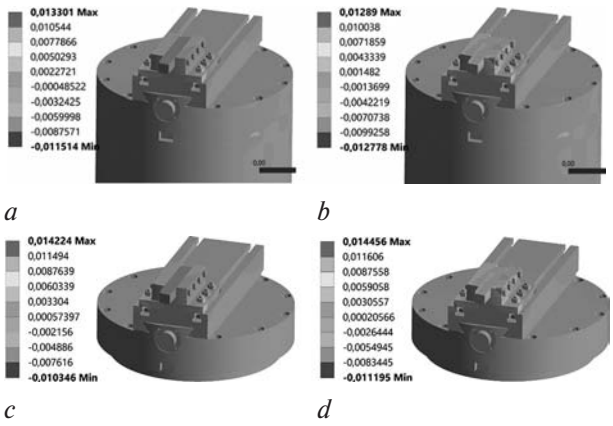

Figure 11 — Distribution of displacements ux after the first loading step (bolts pretension): *a — FN*; *b — F*; *c — HN*; *d — H*, mm

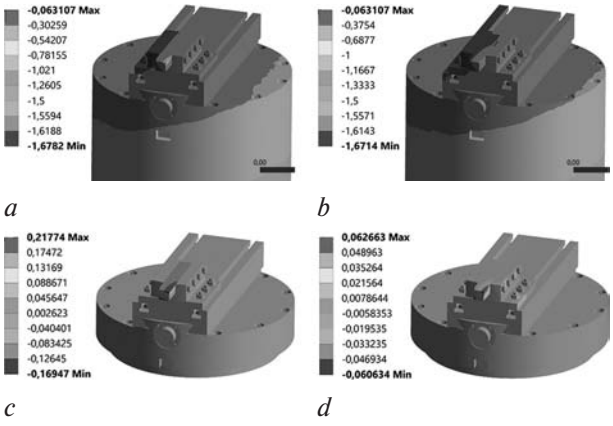

Figure 12 — Distribution of displacements ux after the second loading step (cutting): *a — FN*; *b — F*; *c — HN*; *d — H*, mm

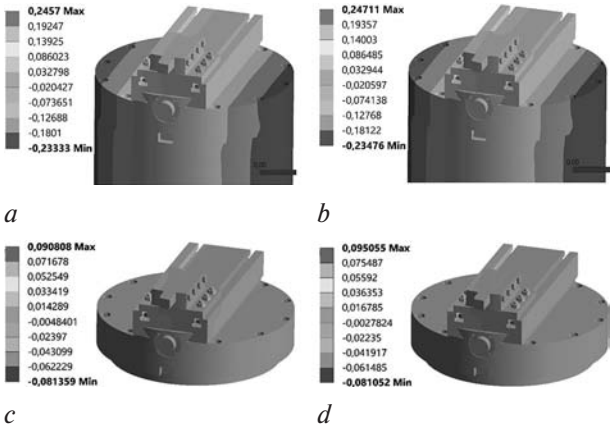

Figure 13 — Distribution of displacements uy after the first loading step (bolts pretension): *a — FN*; *b — F*; *c — HN*; *d — H*, mm

The total displacements of the cutter after bolts pretension are 5,85 mm and 5,95 mm for *FN* and *F* calculations, respectively.

The total displacements of the cutter during cutting are 11,01 mm and 11,04 mm for the *FN* and *F* calculations, respectively.

In calculations *HN* and *H* the absolute values of maximal u_z displacements are 0,07 mm and 0,11 mm after bolts pretension, 0,02 mm and 0,34 mm during cutting respectively (see figures 15, 16).

The total displacements of the cutter after bolts pretension are 0,26 mm and 0,15 mm for the calculations *HN* and *H* respectively.

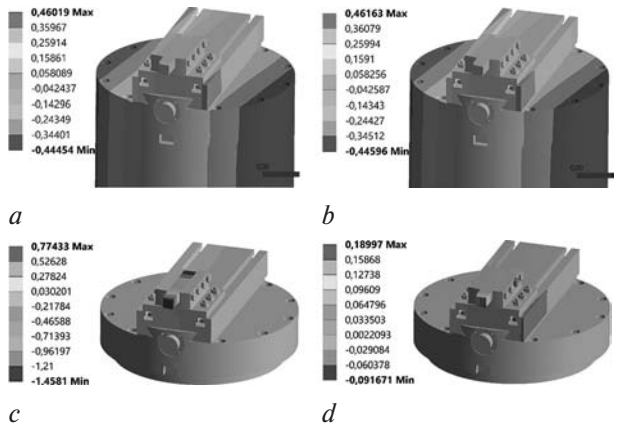

Figure 14 — Distribution of displacements uy after the second loading step (cutting): *a — FN*; *b — F*; *c — HN*; *d — H*, mm

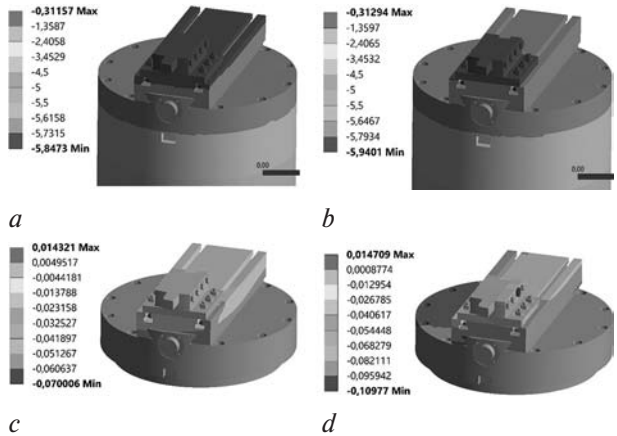

Figure 15 — Distribution of displacements uz after the first loading step (bolts pretension): *a — FN*; *b — F*; *c — HN*; *d — H*, mm

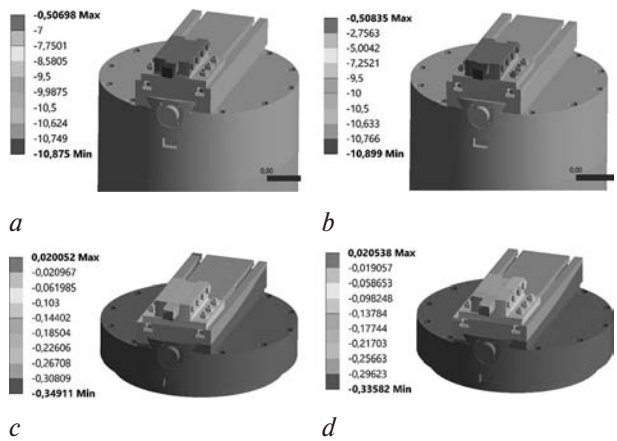

Figure 16 — Distribution of displacements uz after the second loading step (cutting): *a — FN*; *b — F*; *c — HN*; *d — H*, mm

The total displacements of the cutter during cutting are 1,51 mm and 0,39 mm for the *HN* calculation *H* respectively.

Thus, gravity has a significant (about 53 %) impact on maximal deflection of the boring bar.

In calculations without boring bar the bolts pretension together with gravity force contribute up to 17 % and up to 37 % in total deflection of the cutter, upper, middle and lower supports in calculations *HN* and *H* respectively.

Conclusion. Mechanical and mathematical models allowing description of the three-dimensional stress-strain state of the boring bar front-end support structure of heavy-duty horizontal boring lathe were developed. Contact problems for the elements of the boring bar front-end support multi-element system were formulated. The effect of the bolts pretension on the upper support was studied. The effect of boring bar bending on the stress-strain state of supports was analyzed.

Computer modeling based on finite element method was made for the boring bar front-end support system considering multiple contact interactions of its elements, bolts pretension, cutting process and non-contact deformation due to boring bar bending.

Four different statements of the problem were developed and analyzed. They showed how the stress-strain state of the system was influenced by bolts pretension clamping cutter and boring bar bending due to the gravitational force.

In general, it should be noted that both bolts pretension of bolted connections *A* and *B* and cutting process had strong impact on stress-strain state of the upper support in the area of cutter fastening. At the same time, the middle support had the same von-Mises stresses and strains after bolts pretension of group *B* bolts and during cutting. It was shown that even under absent bolts pretension of group *A* bolts the cutter was held in the upper support during the cutting.

The carried out analysis showed that the components of the stress-strain state of the studied system had similar distributions (maximal von-Mises stresses in the cutting region vary from 1,71 GPa to 1,72 GPa for all calculations) regardless to the boring bar bending by virtue of the Saint-Venant principle. Boring bar bending had significant influence only on the displacements.

Gravity had significant (about 54 %) impact on the maximal deflection of the boring bar in *z* direction. Displacements u_x and u_y made insignificant contribution to the total deflection of the boring bar.

In calculations without boring bar the bolts pretension and force of gravity contributed up to 17 % and up to 37 % to total deflection of the cutter, upper, middle and lower supports in calculations *HN* and *H* respectively.

Stress concentrators were present in many regions of the contacting bodies. This complicated the analysis of complex distributions of stresses and strains fields. This demonstrates the need to move from the analysis of local characteristics of damageability (stress tensor components) to the analysis of integral ones — dangerous volumes [4, 13–17].

This work was supported by National special project for international scientific and technological cooperation of the People's Republic of China (2012DFR70840).

References

1. Sosnovskiy L.A. *Fundamentals of Tribo-Fatigue*. Gomel, BelSUT, 2003, vol. 1, 246 p.; vol. 2. 234 p. (in Russian).
2. Sosnovskiy L.A. Tribo-Fatigue. Wear-Fatigue Damage and Its Prediction. *Foundations of Engineering Mechanics*, Springer, 2005. 424 p.
3. 摩擦疲劳学 磨损 — 疲劳损伤及其预测. L.A. 索斯洛-夫斯基著, 高万振译 — 中国矿业大学出版社, 2013. 324 p. (in Chinese)
4. Sherbakov S.S., Sosnovskiy L.A. *Mehanika tribofaticheskih sistem* [Mechanics of tribo-fatigue systems]. Minsk, BGU, 2011. 407 p. (in Russian)
5. Sosnovskiy L.A., Sherbakov S.S. *Mechanothermodynamics*. Springer, 2016. 155 p
6. Sosnovskii L.A., Komissarov V.V., Shcherbakov S.S. A Method of Experimental Study of Friction in a Active System. *Journal of Friction and Wear*, 2012, vol. 33, no. 2, pp. 136–145.
7. Zhuravkov M.A., Sherbakov S.S., Krupoderov A.V. Modeling of volumetric damage of multielement clamp-knife-base tribo-fatigue system. ZAMM doi:10.1002/zamm.201500294
8. Sosnovskiy L.A., Bogdanovich A.V., Yelovoy O.M., Tyurin S.A., Komissarov V.V., Sherbakov S.S. Methods and main results of Tribo-Fatigue tests. *International Journal of Fatigue*, 2014, vol. 66, pp. 207–219.
9. Sherbakov S.S., Zhuravkov M.A. Interaction of Several Bodies as Applied to Solving Tribo-Fatigue Problems. *ActaMechanica*, 2013, vol. 224, no. 3, pp. 1541–1553.
10. GOST 4543-71. *Prokat iz legirovannoj konstrukcionnoj stali. Tehnicheskie uslovija* [State Standard 4543-71. Rolling from alloyed structural steel. Technical conditions]. 1973. 39 p. (in Russian)
11. Birger I.A., Iosilevich G.B. *Rezbovye i flancevye soedinenija* [Threaded and flanged connections]. Moscow, Mashinostroenie, 1990. 368 p. (in Russian)
12. ISO 965-2. *ISO general purpose metric screw threads – Tolerances – Part 2: Limits of sizes for general purpose external and internal screw threads – Medium quality. 1998-12-15.* 8 p.
13. Shcherbakov S.S. Modeling of the damaged state by the finite-element method on simultaneous action of contact and noncontact loads. *Journal of Engineering Physics and Thermophysics*, 2012, vol. 85, no. 2. pp. 472–477.
14. Sosnovskiy L.A., Sherbakov S.S. Vibro-impact in rolling contact. *Journal of Sound and Vibration*, 2007, vol. 308, no. 3–5, pp. 489–503.
15. Sherbakov S.S. State of Volumetric Damage of Tribo-Fatigue System. *Strength of Materials*, 2013, vol. 45, no. 2. pp. 171–178.
16. Sosnovskiy L.A., Sherbakov S.S. Mechanothermodynamic Entropy and Analysis of Damage State of Complex Systems. *Entropy*, 2016, vol 18(7), pp.1–34.
17. Sosnovskiy L.A., Sherbakov S.S. Mechanothermodynamical system and its behavior. *Continuum Mech. Thermodyn.*, 2012, vol.24, no. 3, pp. 239–256.

С.С. ЩЕРБАКОВ, д-р физ.-мат. наук, доц.
профессор кафедры теоретической и прикладной механики[1]
E-mail: sherbakovss@mail.ru

ШИ У, доц.
доцент факультета машиностроения и энергетики[2]
E-mail: wushi971819@163.com

ЦЗЮНЬПЭН Шао, проф.
декан факультета машиностроения и энергетики[2]
E-mail: sjp566@hrbust.edu.cn

О.А. НАСАНЬ
младший научный сотрудник[1]
E-mail: nasan_o@mail.ru

[1]Белорусский государственный университет, г. Минск, Республика Беларусь
[2]Харбинский университет науки и технологий, г. Харбин, Китай

Поступила в редакцию 05.07.2017.

ПРОСТРАНСТВЕННОЕ НАПРЯЖЕННО-ДЕФОРМИРОВАННОЕ СОСТОЯНИЕ РАСТОЧНОЙ ОПРАВКИ ШПИНДЕЛЯ СВЕРХНАГРУЖЕННОГО ГОРИЗОНТАЛЬНО-РАСТОЧНОГО СТАНКА

Разработаны механические и математические модели, описывающие пространственное напряженно-деформированное состояние и контактные взаимодействия с трением между упругими элементами расточной оправки шпинделя сверхпрочного горизонтально-расточного станка. Все вычисления были выполнены с использованием пакета конечно-элементного моделирования ANSYS Workbench Mechanical. Рассмотрена статическая постановка задачи с учетом силы тяжести и нелинейного поведения материалов вблизи режущей поверхности инструмента. Проанализированы четыре различных варианта постановки задачи, иллюстрирующие влияние усилий затяжки болтовых соединений, прижимающих режущий инструмент, на напряженно-деформированное состояние системы. Исследовано влияние нагрузки расточной оправки на шпиндель во время резки. Проанализировано влияние изгиба шпинделя на расточную оправку. Проведенный анализ показал, что компоненты напряженно-деформированного состояния исследуемых систем имеют схожие распределения, независимо от изгиба шпинделя из-за силы тяжести. Изгиб шпинделя оказывает существенное влияние только на перемещения. Во многих местах изучаемой системы присутствовали концентраторы напряжений. Это осложнило анализ сложных распределений напряжений и полей напряжений и деформаций. Полученные результаты демонстрируют необходимость перехода от локальных характеристик повреждаемости (компонентов тензора напряжений) к интегральным — опасным объемам.

Ключевые слова: *трибофатика, многоэлементная система, напряженно-деформированное состояние, конечно-элементное моделирование, сверхнагруженный расточный станок, шпиндель, расточная оправка*

Список литературы

1. Сосновский, Л.А. Основы трибофатики / Л.А. Сосновский. — Гомель: БелГУТ, 2003. — Т. 1. — 246 с.; Т. 2. — 234 с.
2. Сосновский, Л.А. Трибофатика. Износоусталостные повреждения и их прогнозирование / Л.А. Сосновский. — Шпрингер, 2005. — 424 с. (англ.)
3. Сосновский, Л.А. Трибофатика. Износоусталостные повреждения и их прогнозирование. / Л.А, Сосновский, пер. Гао Ванчжен. — Китайский университет горного дела и технологий, 2013. — 324 с. (кит.)
4. Щербаков, С.С. Механика трибофатических систем / С.С. Щербаков, Л.А. Сосновский. — Минск: БГУ, 2011. — 407 с.
5. Сосновский, Л.А. Механотермодинамика / Л.А. Сосновский, С.С. Щербаков. — Шпрингер, 2016. — 155 с. (англ.)
6. Сосновский, Л.А. Метод экспериментального исследования трения в силовой системе / Л.А. Сосновский, В.В. Комиссаров, С.С. Щербаков // Трение и износ. — 2012, –Т. 33, № 2. — С. 136–145. (англ.)
7. Журавков, М.А. Моделирование объемной повреждаемости многоэлементной трибофатической системы «прижим — нож — основание» / М.А. Журавков, С.С. Щербаков, А.В. Круподеров // Журнал прикладной математики и механики. — 2017. — Т. 97, № 1. — С. 60–69. (англ.)
8. Методы и основные результаты трибофатических испытаний / Л.А. Сосновский [и др.] // Международный журнал усталости. — 2014. — Т. 66. — С. 207–219. (англ.)
9. Щербаков, С.С. Взаимодействие нескольких тел применительно к задачам трибофатики / С.С. Щербаков, М.А. Журавков // Акта Механика. — 2013. — Т. 224, №3. — С. 1541–1553. (англ.)
10. Прокат из легированной стали. Технические условия: ГОСТ 4543-71. — М.: ИПК Издательство стандартов, 1973. — 39 с.
11. Биргер, И.А. Резьбовые и фланцевые соединения / И.А. Биргер, Г.Б. Иосилевич. — М.: Машиностроение, 1990. — 368 с.
12. ИСО 965-2: ИСО метрические резьбы общего назначения — Допуски — Часть 2: Пределы размеров для внешней и внутренней резьбы общего назначения – Среднее качество. 1998-12-15. — 8 с.
13. Щербаков, С.С. Моделирование состояния повреждаемости методом конечных элементов при одновременном воздействии контактных и неконтактных нагрузок / С.С. Щербаков // Инженерно-физический журнал. — 2012. — Т. 85, № 2. — С. 472–477. (англ.)
14. Сосновский, Л.А. Виброудар при трении качения / Л.А. Сосновский, С.С. Щербаков // Журнал звука и вибрации. — 2007. — Т. 308, Вып. 3–5. — С. 489–503. (англ.)
15. Щербаков, С.С. Состояние объемной повреждаемости трибофатической системы / С.С. Щербаков // Проблемы прочности. — 2013. — Т. 45, № 2. — С. 171–178. (англ.)
16. Сосновский, Л.А. Механотермодинамическая энтропия и анализ состояния поврежденности сложных систем / Л.А. Сосновский, С.С. Щербаков // Энтропия. — 2016. — Т. 18(7), 268. — С. 1–34. (англ.)
17. Сосновский, Л.А. Механотермодинамическая система и ее поведение / Л.А. Сосновский // Механика сплошных сред и термодинамика. — 2012. —Т. 24, Вып. 3. — С. 239–256. (англ.)